

## Supplementary Information

### **Emulsion droplets-enabled selective electrochemical oxidation of alcohols at industrially relevant current densities**

*Menglu Cai<sup>1</sup> | Shenyuan Gao<sup>1</sup> | Haoqiong Zhu<sup>1</sup> | Xiaozhong Wang<sup>1, 2</sup> | Gang Xu<sup>1\*</sup> | Liyan Dai<sup>1, 2\*</sup>*

#### **This PDF file includes:**

Supplementary Note 1 to 2

Supplementary Fig. 1 to Supplementary Fig. 46

Supplementary Table 1 to Supplementary Table 3

## Table of Contents

Supplementary Note 1   Methods .....	4
Figure S1   Standard curve of benzaldehyde.....	6
Figure S2   Standard curve of p-chlorobenzaldehyde. ....	7
Figure S3   Standard curve of p-methylbenzaldehyde. ....	7
Figure S4   Standard curve of Vanillin.....	8
Figure S5   Standard curve of 2-Furaldehyde.....	8
Figure S6   Standard curve of 3-Pyridinecarboxaldehyde.....	9
Figure S7   Standard curve of acetophenone.....	9
Figure S8   Standard curve of Cyclohexanone. ....	10
Supplementary Note 2   Calculations of energy consumption in various NaCl concentration .....	14
Table S1   The effect of electrolyte on electrochemical oxidation of benzyl alcohol ..	15
Figure S9   Effect of the electrolyte composition on benzaldehyde yield.....	15
Table S2   The structure parameters of TEMPO-Silica and Silica.....	16
Table S3   The comparison of the performance in this work with other established literature in electrochemical benzaldehyde synthesis form benzyl alcohol. ....	17
Figure S10   The photos of the undivided cell. ....	18
Figure S11   The screening of the organic solvent in the reaction. ....	19
Figure S12   The linear sweep voltammograms of various anode materials.....	19
Figure S13   Emulsion formation at different stirring rates. ....	20
Figure S14   Changes in benzaldehyde conversion and selectivity at different stirring speeds .....	20
Figure S15   The v-t curves at different stirring rates. ....	21
Figure S16   The resistance in different electrolyte at 600 rpm .....	22
Figure S17   The photograph of the electrolyte containing different proportions of CH <sub>2</sub> Cl <sub>2</sub> .....	23
Figure S18   The gas chromatogram for benzyl alcohol oxidation reaction in high CH <sub>2</sub> Cl <sub>2</sub> content .....	23
Figure S19   Changes in benzaldehyde yield and reaction voltage at different NaCl concentrations .....	24
Figure S20   FI-IR spectra with breakpoints of Silica and TEMPO-Silica .....	25
Figure S21   The XPS survey spectrum of TEMPO-Silica and Silica .....	26
Figure S22   The pore size distribution of Silica and TEMPO-Silica. ....	27

Figure S23   Characterization of Silica and TEMPO-Silica.....	28
Figure S24   Characterization of reused TEMPO-Silica. ....	29
Figure S25  The voltage-time curve during the electrolyte recycling. ....	30
Figure S26   Morphology characterization of fresh Ru-IrO <sub>2</sub> -DSA anode.....	31
Figure S27   Morphology characterization of used Ru-IrO <sub>2</sub> -DSA anode .....	32
Figure S28   N <sub>2</sub> -treated experiment and halogen-free experiment.....	33
Figure S29   The linear sweep voltammograms of DSA.....	34
Figure S30   GC-MS of benzaldehyde. ....	35
Figure S31   Gas chromatogram for benzyl alcohol oxidation at standard reaction condition.....	35
Figure S32   Gas chromatogram for benzyl alcohol oxidation reaction with an increased charge .....	36
Figure S33  <sup>1</sup> H NMR of product in the extracted solution.....	37
Figure S34   GC-MS of p-chlorobenzaldehyde.....	38
Figure S35   Gas chromatogram for p-Chlorobenzyl alcohol oxidation at standard reaction condition.....	38
Figure S36   GC-MS of p-methylbenzaldehyde.....	39
Figure S37   GC-MS of Vanillin. ....	39
Figure S38   GC-MS of 2-Furaldehyde.....	40
Figure S39   Gas chromatogram for Furfuryl alcohol oxidation at standard reaction condition.....	40
Figure S40   GC-MS of 2-Thenaldehyde. ....	41
Figure S41   GC-MS of 5-Chlorothiophene-2-carbaldehyde. ....	41
Figure S42   GC-MS of 5-Bromo-2-thiophenecarbaldehyde. ....	42
Figure S43   GC-MS of 3-Pyridinecarboxaldehyde. ....	43
Figure S44   Gas chromatogram for 3-Pyridinemethanol oxidation at standard reaction condition.....	43
Figure S45   GC-MS of acetophenone. ....	44
Figure S46   GC-MS of Cyclohexanone. ....	44
Reference.....	45

## Supplementary Note 1 | Methods

### Materials, chemicals, and characterization methods

All reagents and chemicals were obtained from commercial sources and were used without any further purification. The Ru-IrO<sub>2</sub>-DSA electrode (thickness 1 mm, 10 mm×20 mm) used for anode was purchased from Shengmolong. The nickel foam (thickness 1 mm, 10 mm×20 mm) electrode used as cathode. Sodium bromide (NaBr, 99%), sodium chloride (NaCl, 99.5%), Sodium thiosulfate (Na<sub>2</sub>S<sub>2</sub>O<sub>3</sub>, 99%) and dichloromethane (CH<sub>2</sub>Cl<sub>2</sub>, 99.5%) were purchased from Sinopharm Chemical Reagent Co. Ltd. (Shanghai, China). Benzyl alcohol (98%) and benzaldehyde (98%) were purchased from Shanghai D&B Biological Science and Technology Co. Ltd. (Shanghai, China). 2,2,6,6-Tetramethylpiperidine-N-oxyl (TEMPO) (98%) is purchased from Bide Pharmatech Co. Ltd. (Shanghai, China). The deionized (DI) water with a resistivity of 18.2 MΩ cm was provided by a Millipore Milli-Q grade.

The morphologies of the materials were characterized by scanning electron microscopy (SEM, Thermo Fisher Scientific, Scios2 Hivac) equipped with an Oxford Xplore 50 EDX detector. The Fourier-transform infrared spectra (FT-IR) was recorded using a Thermo Nicolet iS5 spectrometer (Thermo Fisher). The surface chemical composition of prepared samples was analyzed by X-ray photoelectron spectroscopy (XPS, Thermo Fisher Escalab 250Xi) with Al K $\alpha$  radiation (1486.6 eV). The C 1s peak at 284.8 eV was used as the reference for binding energy calibration. The Brunauer–Emmett–Teller (BET) surface areas were measured using a Micromeritics ASAP 2460 analyzer via nitrogen adsorption, and the pore size distribution was determined using the Horvath–Kawazoe (HK) and BJH method. The bromine concentration was quantified by ICP-MS (Agilent 7800) after acid digestion and a 500-fold dilution of the sample.

The linear sweep voltammetry (LSV) was conducted on a three-electrode setup with Ag/AgCl (3 M KCl) as the reference electrode at a scan rate of 20 mV/s (CHI 760E potentiostat). The EIS measurements were carried out from 100,000 to 0.1 Hz in reaction solution at open circuit voltage.

The reaction yields were calculated by gas chromatography (GC, Agilent 8890 equipped with an SE-54 column) using ethylbenzene as the internal standard. After each reaction, the anode and cathode electrodes were rinsed with dichloromethane, and a certain amount of Na<sub>2</sub>S<sub>2</sub>O<sub>3</sub> was added to quench the reaction. Subsequently, CH<sub>2</sub>Cl<sub>2</sub> was added and the mixture was vigorously stirred, followed by phase separation. The organic phase was collected for yield (Eq. 1) and selectivity (Eq. 2) analysis by GC. The product was confirmed by comparison with standards or gas chromatography-mass spectrometry (GC-MS Agilent 8890-5977B). And the Faraday efficiency was calculated according to Eq. 3.

$$Yield (\%) = \frac{\text{Formed product (mmol)}}{\text{Initial substrate (mmol)}} \times 100 \% \quad (1)$$

$$Selectivity (\%) = \frac{\text{Formed product (mmol)}}{\text{Consumed substrate (mmol)}} \times 100 \% \quad (2)$$

$$Faraday\ efficiency (\%) = \frac{\text{Target product (mol)} \times 2 \times F}{Q} \times 100 \% \quad (3)$$

where  $F$  is the Faradaic constant of 96485 C·mol<sup>-1</sup>,  $Q$  is the total passed charge.

### **Standard curve calculation**

The moles of target product ( $n_{target\ product}$ ) were determined by GC using ethylbenzene as internal standard.

Standard curve of benzaldehyde was calculated as followed:

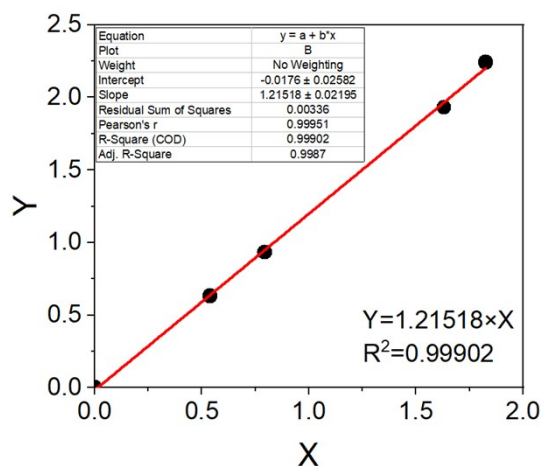


**Figure S1 | Standard curve of benzaldehyde.**

Standard curve of benzaldehyde

$$Y=1.21518X$$

Where X represents the peak area ratio of benzaldehyde to ethylbenzene, an Y represents the molar ratio of benzaldehyde to ethylbenzene. Several solutions with various concentration of benzaldehyde were carried out for linear fitting of standard curve.

Other products standard curves are as follows:

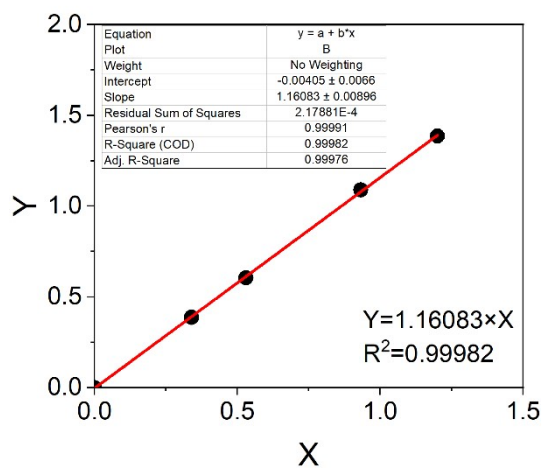


Figure S2 | Standard curve of p-chlorobenzaldehyde.

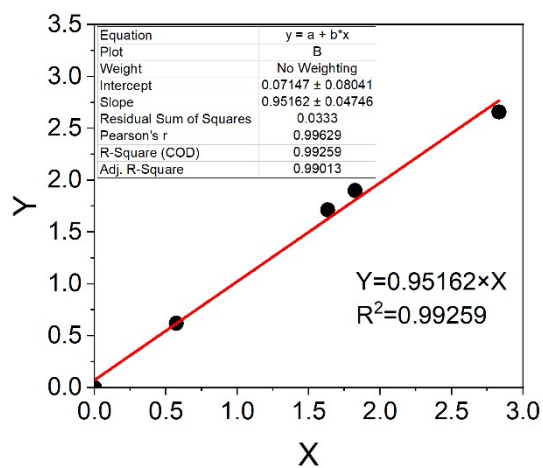
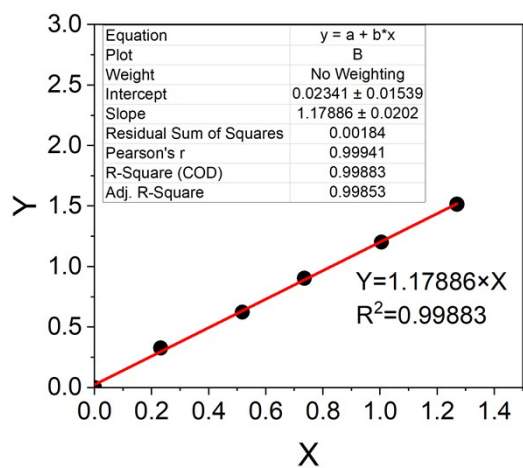
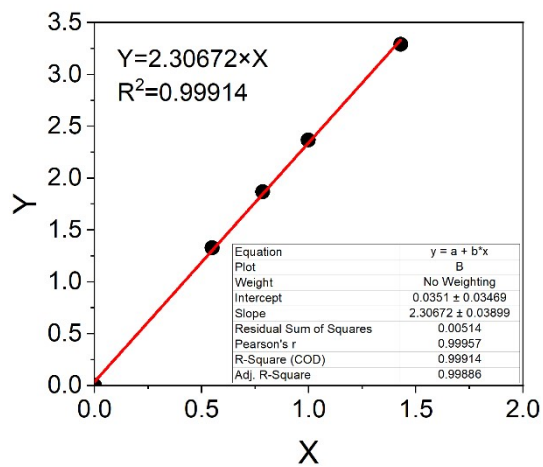


Figure S3 | Standard curve of p-methylbenzaldehyde.



**Figure S4 | Standard curve of Vanillin.**



**Figure S5 | Standard curve of 2-Furaldehyde.**

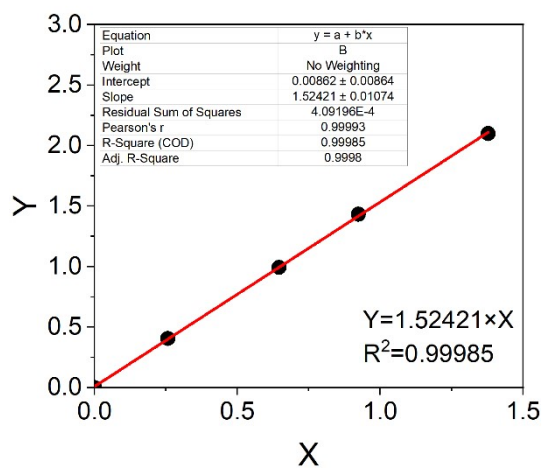


**Figure S6 | Standard curve of 3-Pyridinecarboxaldehyde.**

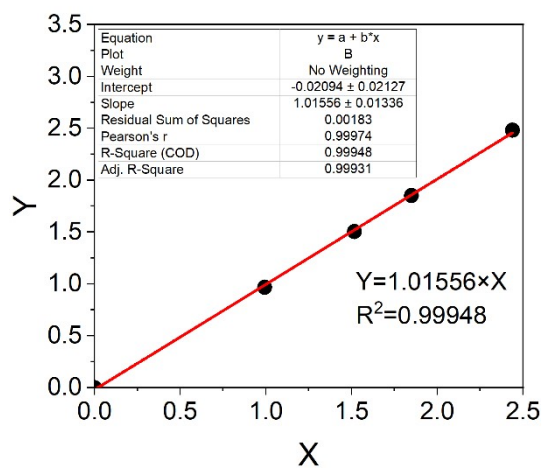


**Figure S7 | Standard curve of acetophenone.**

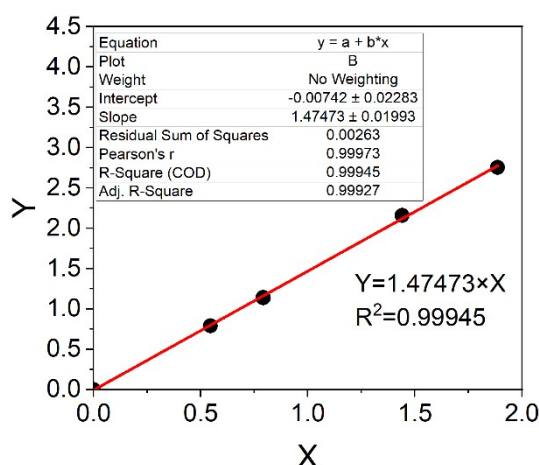


**Figure S8 | Standard curve of Cyclohexanone.**

### **Preparation procedure for TEMPO-Silica catalyst**

For TEMPO-Silica catalyst was prepared followed the previously reported procedure.<sup>[1,2]</sup> Specifically, (3-aminopropyl)triethoxysilane (APTES, 885.5 mg, 4 mmol), methanol (8.5 mL), and 4-oxo-2,2,6,6-tetramethylpiperidinoxy (4-oxo-TEMPO, 780.4 mg, 4.6 mmol) were sequentially added to a 100 mL round-bottom flask. The mixture was stirred vigorously at room temperature for 2 h to ensure complete mixing. Then, sodium cyanoborohydride (377.0 mg, 6 mmol) was added, and the reaction was continued for 12 hours to promote the reductive amination of 4-oxo-TEMPO, forming the coupling intermediates. Concentrated HCl (38%) was slowly added dropwise to adjust the pH of the solution to 3-4. Fresh silica gel (2g, average particle size 40-60  $\mu\text{m}$ , pore size 6 nm) was then introduced, and the suspension was stirred gently for 24 h. The resulting solid was collected by centrifuged, and the solid was washed with dichloromethane for three times. The crude product solid was placed in a Soxhlet extractor and continuously washed with dichloromethane as an extractant for 24 hours to remove the unbound TEMPO. Finally, the obtained solid was dried under vacuum at 40°C for 12 h to afford the silicon-supported TEMPO catalyst, which was denoted as TEMPO-Silica.

## **Procedure for electrosynthesis of aldehydes**

The highly selective electrochemical oxidation of alcohols was investigated using the oxidation of benzyl alcohol to benzaldehyde as a model reaction. The experiments were conducted in a 30 mL straight-neck electrolytic cell with an inner diameter of 26 mm and a height of 60 mm (Figure S10). The reaction procedure was as follows: benzyl alcohol (0.5 mmol, 54 mg), TEMPO (5 mol% of substrate, 4 mg), and CH<sub>2</sub>Cl<sub>2</sub> (1 mL) were successively added to the reactor, followed by addition of 14 mL aqueous solution containing 3 M NaCl and 0.01 M NaBr. Then a magnetic bar was added and the mixture was rapidly stirred (600 rpm) until a uniform emulsion was formed.

Nickel foam (1 mm thick) was used as the cathode. Before use, the electrode was washed with 2 mol·L<sup>-1</sup> hydrochloric acid to remove the surface oxide layer, followed by sequential rinsing with water and ethanol. The DSA (Ru-IrO<sub>2</sub>/Ti) anode and the nickel foam cathode were then fixed on a platinum electrode and immersed in the reaction solution, ensuring an effective geometric area of 1 cm<sup>2</sup>. Then, the magnetic stirring was turned on (600 rpm), and a DC regulated power supply was connected to perform constant current electrolysis at a current density of 100 mA·cm<sup>-2</sup> (which means when 100 mA is applied, the immersion area of the electrode before stirring is 1 cm<sup>2</sup>), and the total charge passed is 2.2 F/mol. After completion of the reaction, the electrode was removed, and sodium sulfite solution was added to quench the remaining oxidative species. Ethylbenzene was added as the internal standard and after a few minutes vigorous stirring, the mixture was allowed to stand for phase separation. The organic phase was collected, diluted, and dried over anhydrous sodium sulfate, followed by analysis using GC. The benzaldehyde yield was quantified using the internal standard method. Unless otherwise specified, the reaction conditions are the same for all other substrates, and the product yield is determined by the internal standard method using ethylbenzene as the internal standard.

When verifying the immobilization performance of TEMPO, 4 mg TEMPO was replaced with 40 mg TEMPO-Silica, while the rest of the experimental procedure remained unchanged.

### **TEMPO-Silica stability test:**

The experiment was performed at a constant current density of 100 mA/cm<sup>2</sup> using a solvent system of 40 mg TEMPO-Silica and 0.5 mmol benzyl alcohol in a mixture of 15 ml CH<sub>2</sub>Cl<sub>2</sub>-H<sub>2</sub>O (1:14 vol%), and 3 M NaCl and 0.01 M NaBr was dissolve in water. After each electrolysis, the TEMPO-Silica catalyst was separated by filtration through a 0.22 μm microporous membrane and subsequently washed three times with deionized water and dichloromethane, respectively. After drying at 40 °C, the catalyst was reused in the next cycle.

Since the catalyst dosage also influence the conversion of benzyl alcohol to benzaldehyde, three parallel experiments were conducted. When a lower yield was observed in the last run, the catalyst from the three groups were combined to obtain a sufficient amount of catalyst for the next cycle, in order to verify whether the material itself had undergone deactivation.

### **Recyclability of electrolyte experiment:**

The experiment was performed at a constant current density of 100 mA/cm<sup>2</sup> using a solvent system of 20 mg TEMPO-Silica and 0.5 mmol benzyl alcohol in a mixture of 15 ml CH<sub>2</sub>Cl<sub>2</sub>-H<sub>2</sub>O (1:14 vol%), and 3 M NaCl and 0.01 M NaBr was dissolve in water. After each electrolysis, the mixture was allowed to stand and then the water and oil phases were separated. The oil phase was used for product yield analysis, while the aqueous phase was replenished with 1 mL of CH<sub>2</sub>Cl<sub>2</sub>, 0.5 mmol of benzyl alcohol, and 20 mg of TEMPO-Silica. We conducted solvent circulation experiments four times based on catalyst circulation results. In each cycle, the organic phase was collected to test the yield of benzaldehyde using GC, while the aqueous phase was retained for the subsequent reaction. At the fourth cycles, the aqueous phase was collected to determine the concentration and moles of bromide using ICP-MS.

### **Inductively coupled plasma-Mass Spectrometry (ICP-MS):**

The concentration and total amounts of Br were determined using an Agilent 7800(MS). Testing parameters were listed below:

Pump rate: 20 r/min;

Nebulizer flow: 1 L/min; Auxiliary gas: 1 L/min;

Sample flush time: 40 s;

RF power: 1550 W.

In this experiment, 1 ml of aqueous phase obtained by extraction was digested by acid, then diluted to a final volume of 25 mL prior to testing. The sample was further diluted 500 times.

## Supplementary Note 2 | Calculations of energy consumption in various NaCl concentration

To calculate the energy consumption, we first list the voltage data and other reaction parameters in the following:

NaCl concentration (M)	Voltage (V)	Time (h)	Yield of benzaldehyde (%)	Faraday efficiency (%)
0.5	3.8	0.295	>99	90.9
1	3.2	0.295	>99	90.9
2	3.0	0.295	>99	90.9
3	2.8	0.295	>99	90.9
4	2.8	0.295	>99	81.8

In each reaction, the initial of benzyl alcohol is 0.5 mmol, and the current is 0.1A. Take 3.0 M NaCl as an example to calculate the energy consumption:

Total energy consumed =  $0.1 \text{ A} \times 2.8 \text{ V} \times 0.295 \text{ h} = 8.26 \times 10^{-5} \text{ kWh}$

Benzaldehyde produced =  $0.5 \text{ mmol} \times 99\% = 0.495 \text{ mmol} = 52.53 \text{ mg}$

Benzyl alcohol to benzaldehyde energy consumption =  $8.26 \times 10^{-5} \text{ kWh} / 52.53 \times 10^{-9} \text{ t} = 1571.39 \text{ kWh/t}$

Based on the above calculations, energy consumption at different concentrations can be obtained, and the data is as follows:

Entry	NaCl concentration (M)	Energy consumption (kWh·t <sup>-1</sup> )
1	0.5	2132.60
2	1	1795.87
3	2	1683.63
4	3	1571.39
5	4	1724.69

When the NaCl concentration ranged from 0.5 M-3 M, the benzaldehyde yield remains above 99%, while energy consumption decreases directly from 2132.6 kWh·t<sup>-1</sup> to 1571.39 kWh·t<sup>-1</sup>. These results indicated that the system can operate efficiently over a wide concentration range, with 3 M NaCl identified as the optimal electrolyte concentration from the perspective of energy consumption.

**Table S1 | The effect of electrolyte on electrochemical oxidation of benzyl alcohol**

Entry	Change condition	Yield (%)	Faraday efficiency (%)
1	<sup>a</sup> Standard	>99.0	90.9
2	No NaCl with 2 M NaBr	85.0	77.2
3	No NaCl and TEMPO	64.4	58.6
4	No NaBr	9.2	8.3
5	No TEMPO	24.0	21.8
6	No electron	0	/
7	0.005M NaBr	>99.0	90.9
8	1.25 mol% TEMPO	92.4	84
9	2.5 mol% TEMPO	>99.0	90.9

<sup>a</sup> Standard condition: benzyl alcohol (0.5 mmol). organic phase: 1 ml CH<sub>2</sub>Cl<sub>2</sub> containing 5 mol% TEMPO. aqueous phase: 14 mL water containing 2 M NaCl and 0.01 M NaBr. Anode: DSA (1 cm<sup>2</sup>). Cathode: Nickel foam (1 cm<sup>2</sup>). Stirring speed is 600 rpm with 20 mA cm<sup>-2</sup>, and the total charge passed is 106.1C.

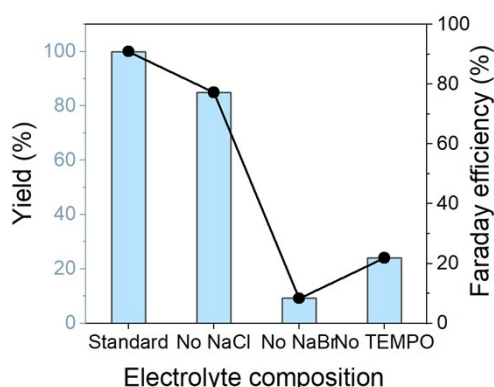


**Figure S9 | Effect of the electrolyte composition on benzaldehyde yield.** Reaction conditions: 0.5 mmol of benzyl alcohol with 5 mol% TEMPO (4 mg). Anode: DSA (1 cm<sup>2</sup>). Cathode: Nickel foam (1 cm<sup>2</sup>). The current density is 100 mA/cm<sup>2</sup> and total charge passed is 2.2 F/mol.

**Table S2 | The structure parameters of TEMPO-Silica and Silica**

Entry	Sample	$S_{\text{BET}}(\text{m}^2/\text{g})^{\text{a}}$	$V_{\text{p}}(\text{cm}^3/\text{g})^{\text{a}}$	PD (nm) <sup>a</sup>
1	Silica	301.1	0.855	10.7
2	TEMPO-silica	259.1	0.606	8.3

<sup>a</sup> Determined from N<sub>2</sub> adsorption-desorption at -195.96 °C and calculated using the BET and BJH methods ( $S_{\text{BET}}$  and  $r_{\text{p}}$ ), t-polt method ( $V_{\text{p}}$ ), respectively.

**Table S3 | The comparison of the performance in this work with other established literature in electrochemical benzaldehyde synthesis from benzyl alcohol.**

Entry	Concentration of benzyl alcohol (M)	Current density (mA/cm <sup>2</sup> )	Productivity (mol/cm <sup>2</sup> /h)	FE(%)	Yield (%)	Ref
1	4	500	79.4	74	87.3	This work
2	0.2	600	0.0073	57.8	98	Green Chem <sup>[3]</sup>
3	8	180	3.24	97	88	Sci. Adv. <sup>[4]</sup>
4	0.4	30	1.954	37	96	Tetrahedron Letters <sup>[5]</sup>
5	0.5	30	5.26	94	94	Journal of Physical Organic Chemistry <sup>[6]</sup>
6	0.2	20	4.78	64	96	J. Org. Chem. <sup>[7]</sup>
7	0.1	200	10.7	95	99.99	AIChE Journal <sup>[8]</sup>

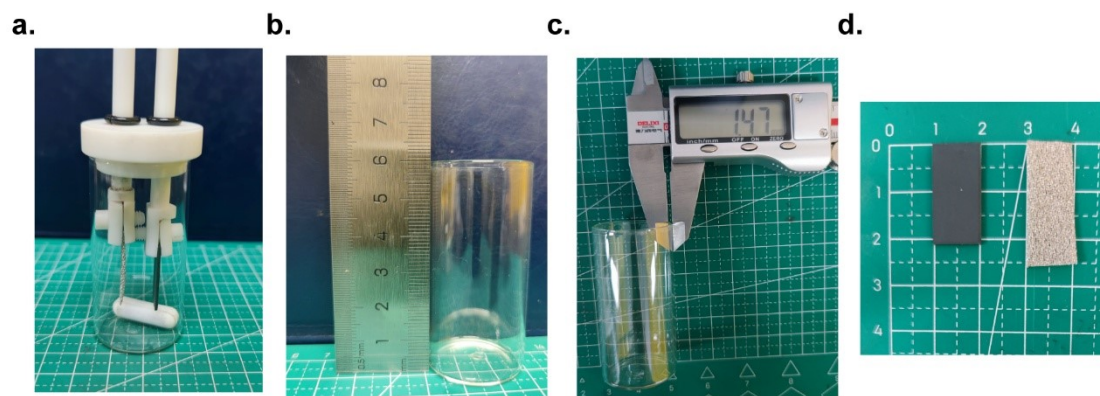


**Figure S10 | The photos of the undivided cell.** a-c) the photos of the reactor. d) the photos of the anode (DSA) and cathode (nickel foam). The experiments were conducted in a 30 mL straight-neck electrolytic cell with an inner diameter of 26 mm and a height of 60 mm.

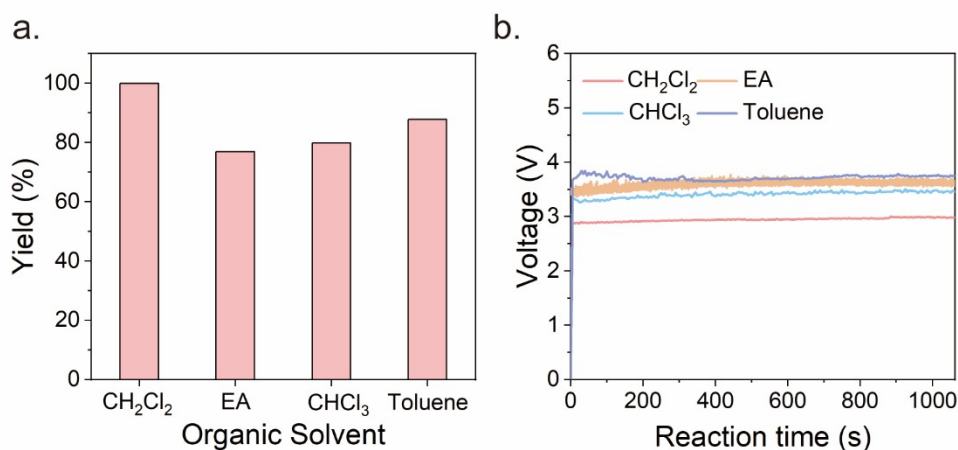


**Figure S11 | The screening of the organic solvent in the reaction.** a) the yield of benzaldehyde in different organic solvent. b) the voltage during the reaction in different organic solvent. Reaction solutions: 0.5 mmol of benzyl alcohol in 1 mL organic solvent with 5 mol% TEMPO (4 mg), then adding 14 mL water with 3M NaCl and 0.01 M NaBr.

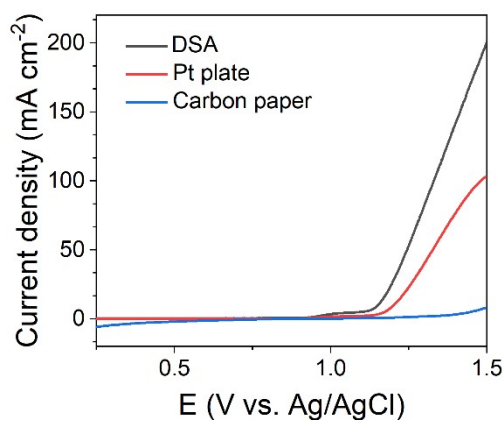


**Figure S12 | The linear sweep voltammograms of various anode materials.** The materials including dimensionally stable anode (DSA), carbon paper (CP) and platinum plate. Analyzed solution: 3 M NaCl and 0.01 M NaBr in 10mL of water solvent. Ag/AgCl was used as reference electrode and nickel foam was used as counter electrode. The scan rate was 20 mV/s.

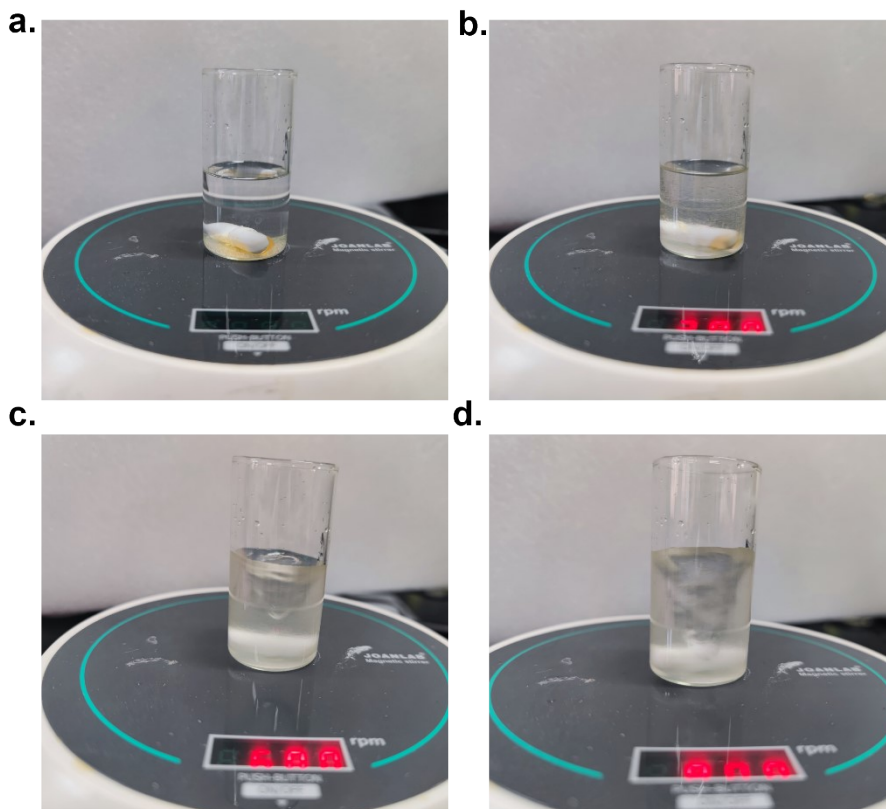


**Figure S13 | Emulsion formation at different stirring rates.** a) 0 rpm. b) 200 rpm. c) 600 rpm. d) 800 rpm. Reaction solutions: 0.5 mmol of benzyl alcohol in 1 mL  $\text{CH}_2\text{Cl}_2$  with 5 mol% TEMPO (4 mg), then adding 14 mL water with 3M NaCl and 0.01 M NaBr.

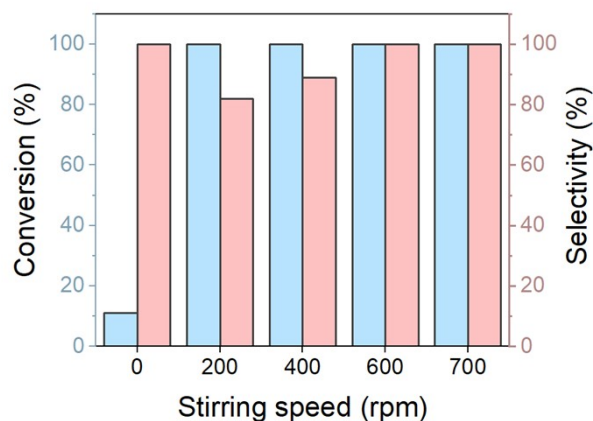


**Figure S14 | Changes in benzaldehyde conversion and selectivity at different stirring speeds.** Reaction conditions: 0.5 mmol of benzyl alcohol in 1 mL  $\text{CH}_2\text{Cl}_2$  with 5 mol% TEMPO (4 mg), then adding 14 mL water with 3M NaCl and 0.01 M NaBr. Anode: DSA (1  $\text{cm}^2$ ). Cathode: Nickel foam (1  $\text{cm}^2$ ). The current density is 100  $\text{mA}/\text{cm}^2$  and the total charge passed is 2.2 F/mol.

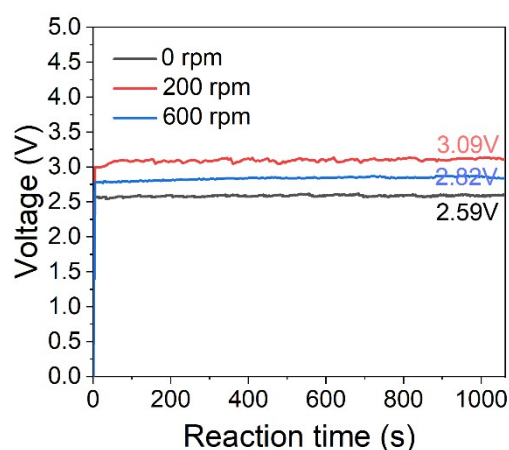


**Figure S15 | The v-t curves at different stirring rates.** Reaction solutions: 0.5 mmol of benzyl alcohol in 1 mL  $\text{CH}_2\text{Cl}_2$  with 5 mol% TEMPO (4 mg), then adding 14 mL water with 3M NaCl and 0.01 M NaBr. Anode: DSA ( $1 \text{ cm}^2$ ). Cathode: Nickel foam ( $1 \text{ cm}^2$ ). The current density is  $100 \text{ mA/cm}^2$  and total charge passed is  $2.2 \text{ F/mol}$ .

Note:

Due to the current and the number of devices limitation of the electrochemical workstation (CHI 760E), most reactions were conducted under DC power. As a result, continuous v-t curves could not be obtained for all experiments. Nevertheless, the initial voltage and the voltage before the end of each experiment was recorded when we use DC power, and the results indicate that the voltage remained relatively stable after the reaction was started, and the voltage presented in DC power is similar to the v-t data recorded by CHI 760E. Therefore, when presenting the voltage data, we report the reaction voltage measured prior to the end of the experiment.

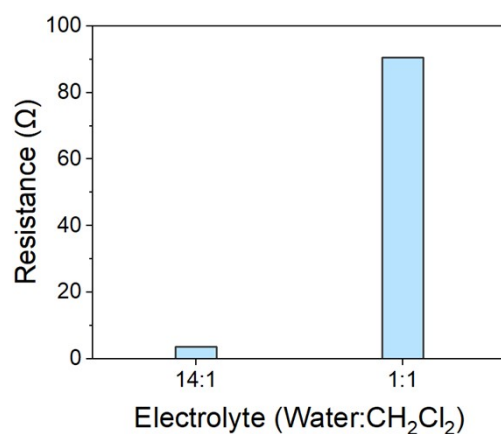


**Figure S16 | The resistance in different electrolyte at 600 rpm.**

Note:

The resistance value was obtained from electrochemical impedance spectroscopy (EIS); specifically, the high-frequency intercept on the real axis of the Nyquist plot corresponds to the solution resistance. The EIS measurements were carried out from 100,000 to 0.1 Hz in reaction solution at open circuit voltage. Reaction solutions: 0.5 mmol of benzyl alcohol in CH<sub>2</sub>Cl<sub>2</sub> with 5 mol% TEMPO (4 mg), then adding water with 3M NaCl and 0.01 M NaBr, the total volume of the aqueous phase and dichloromethane is 15 mL.

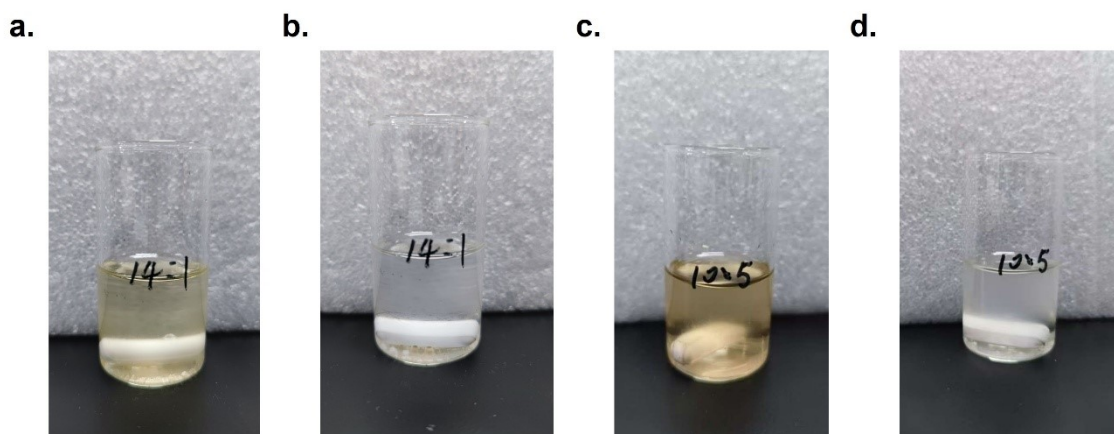


**Figure S17 | The photograph of the electrolyte containing different proportions of  $\text{CH}_2\text{Cl}_2$ .** The photograph of the  $\text{CH}_2\text{Cl}_2$ - $\text{H}_2\text{O}$  (14:1 volume ratio) reaction solution after the reaction is completed (a) and quenched with  $\text{Na}_2\text{S}_2\text{O}_3$  (b). The photograph of the  $\text{CH}_2\text{Cl}_2$ - $\text{H}_2\text{O}$  (10:5 volume ratio) reaction solution after the reaction is completed (c) and quenched with  $\text{Na}_2\text{S}_2\text{O}_3$  (d). Reaction solutions: 0.5 mmol of benzyl alcohol in  $\text{CH}_2\text{Cl}_2$  with 5 mol% TEMPO (4 mg), then adding water with 3M NaCl and 0.01 M NaBr. The total volume of the aqueous phase and dichloromethane is 15 mL. Anode: DSA (1  $\text{cm}^2$ ). Cathode: Nickel foam (1  $\text{cm}^2$ ). The current density is 100  $\text{mA}/\text{cm}^2$  and the total charge passed is 2.2 F/mol.

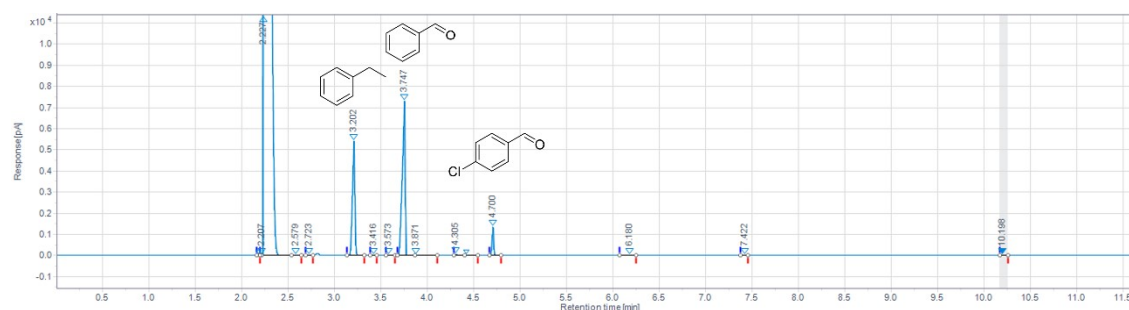


**Figure S18 | The gas chromatogram for benzyl alcohol oxidation reaction in high  $\text{CH}_2\text{Cl}_2$  content.** Reaction solutions: 0.5 mmol of benzyl alcohol in 5 mL  $\text{CH}_2\text{Cl}_2$  with 5 mol% TEMPO (4 mg), then adding 10 mL water with 3M NaCl and 0.01 M NaBr. Anode: DSA (1  $\text{cm}^2$ ). Cathode: Nickel foam (1  $\text{cm}^2$ ). The current density is 100  $\text{mA}/\text{cm}^2$  and the total charge passed is 2.2 F/mol.

Note:

An increase in the proportion of the organic phase resulted in a deeper reddish-brown coloration of the reaction solution after completion of the reaction (Figure S17). Moreover, the formation of halobenzaldehyde (Figure S18) in the products indicate that the generated halogens exhibit higher solubility in the organic phase compared with systems containing a lower organic-phase ratio.

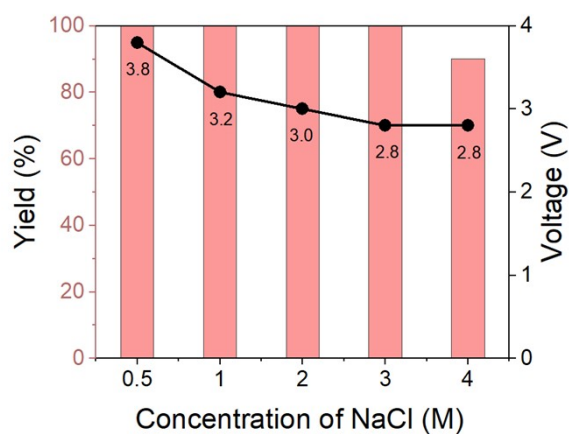


**Figure S19 | Changes in benzaldehyde yield and reaction voltage at different NaCl concentrations.** Reaction conditions: 0.5 mmol of benzyl alcohol in 1 mL CH<sub>2</sub>Cl<sub>2</sub> with 5 mol% TEMPO (4 mg), then adding 14 mL water with various concentration of NaCl and 0.01 M NaBr. Anode: DSA (1 cm<sup>2</sup>). Cathode: Nickel foam (1 cm<sup>2</sup>). Stirring at 600 rpm. The current density is 100 mA/cm<sup>2</sup> and the total charge passed is 2.2 F/mol.

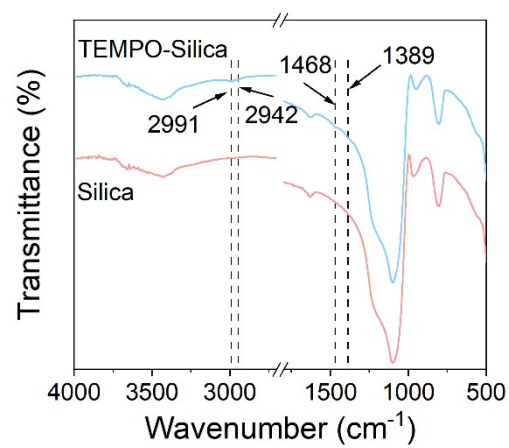


**Figure S20 | FT-IR spectra with breakpoints of Silica and TEMPO-Silica.**

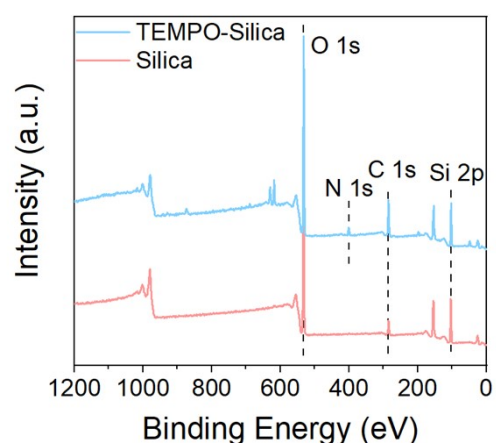


**Figure S21 | The XPS survey spectrum of TEMPO-Silica and Silica.**

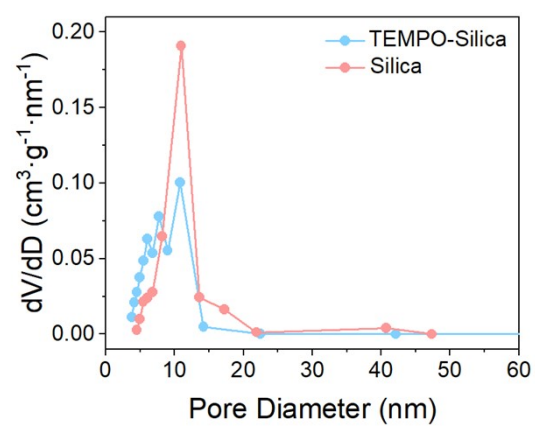


**Figure S22 | The pore size distribution of Silica and TEMPO-Silica.**

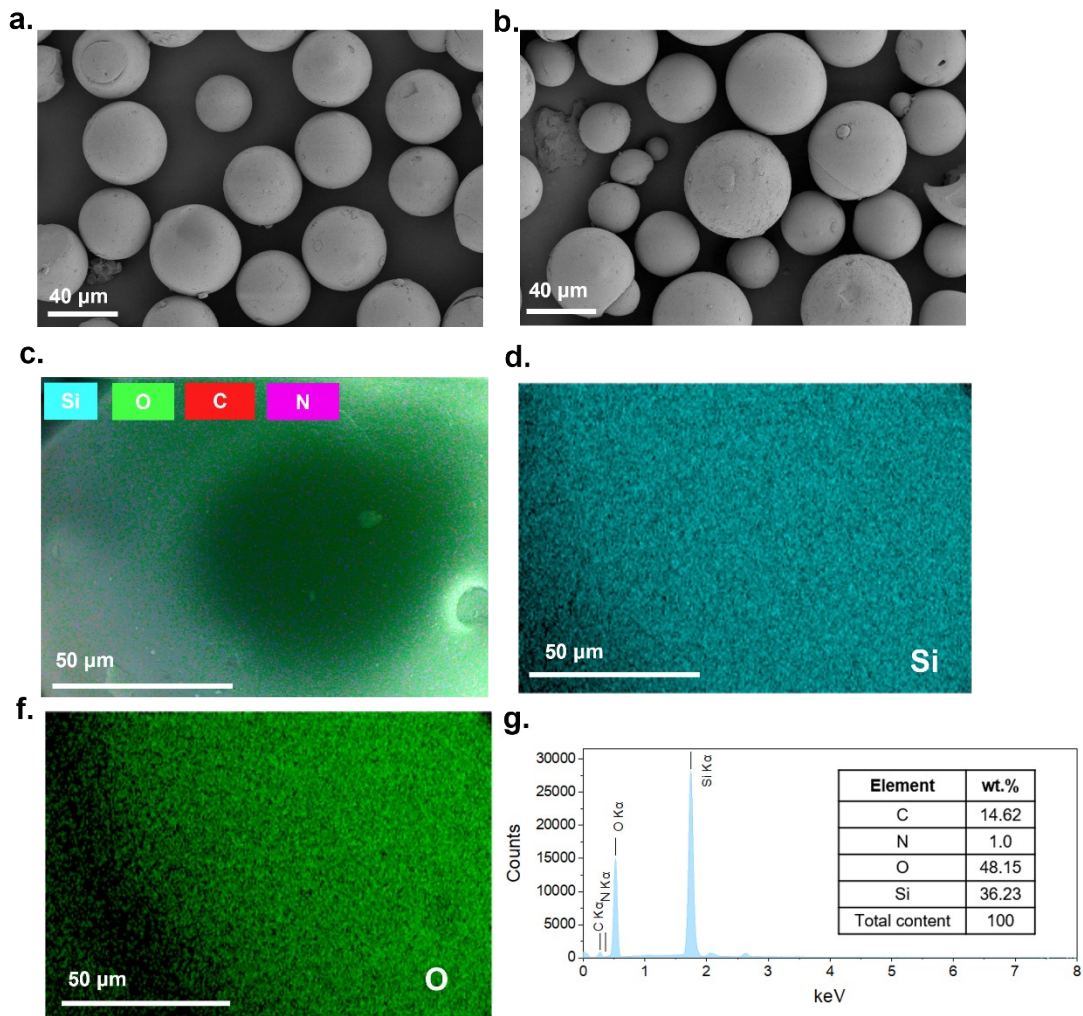


**Figure S23 | Characterization of Silica and TEMPO-Silica.** SEM images of a) Silica and b) TEMPO-Silica. The elemental mapping figures c-f) of TEMPO-Silica, and the g) EDS spectrum and the element content of TEMPO-Silica obtained from Figure S23c. The data in Figure 23g represent the elemental mass content within the scanned area.

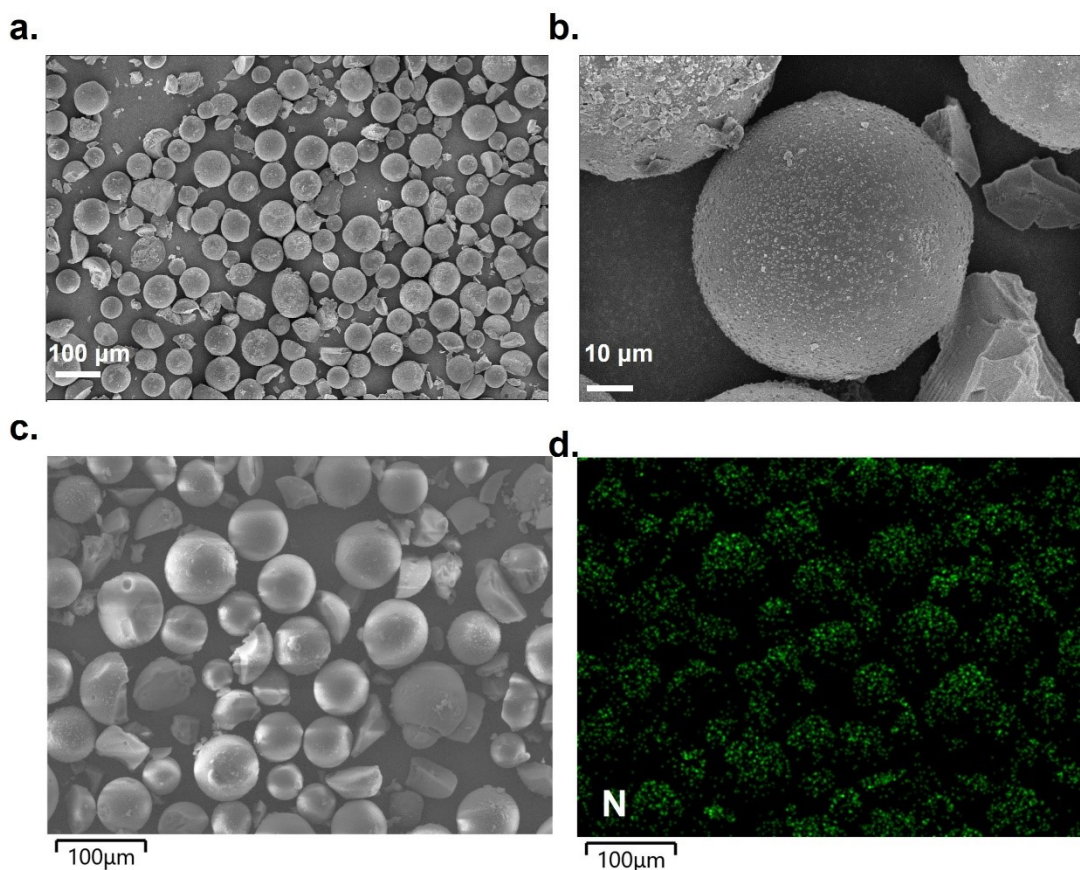


**Figure S24 | Characterization of reused TEMPO-Silica.** a-b) SEM images and c-d) the elemental mapping figures of TEMPO-Silica used for 5 times.

Note:

Morphological characterization of the recycled TEMPO-Silica indicated that, although some small spheres were fractured due to vigorous stirring, the majority retained their original spherical morphology. Elemental mapping further confirmed that N remained uniformly distributed over the material surface, indicating that the material has heterogeneous characteristics.

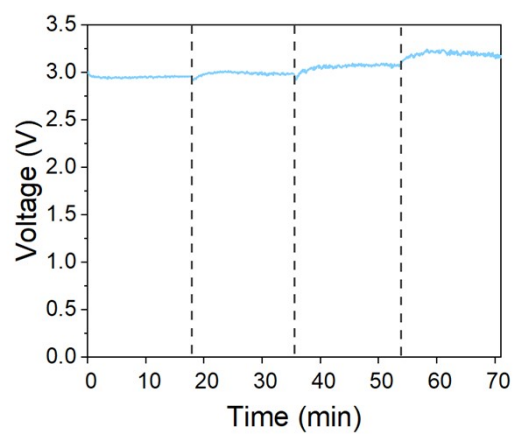


**Figure S25| The voltage-time curve during the electrolyte recycling.**

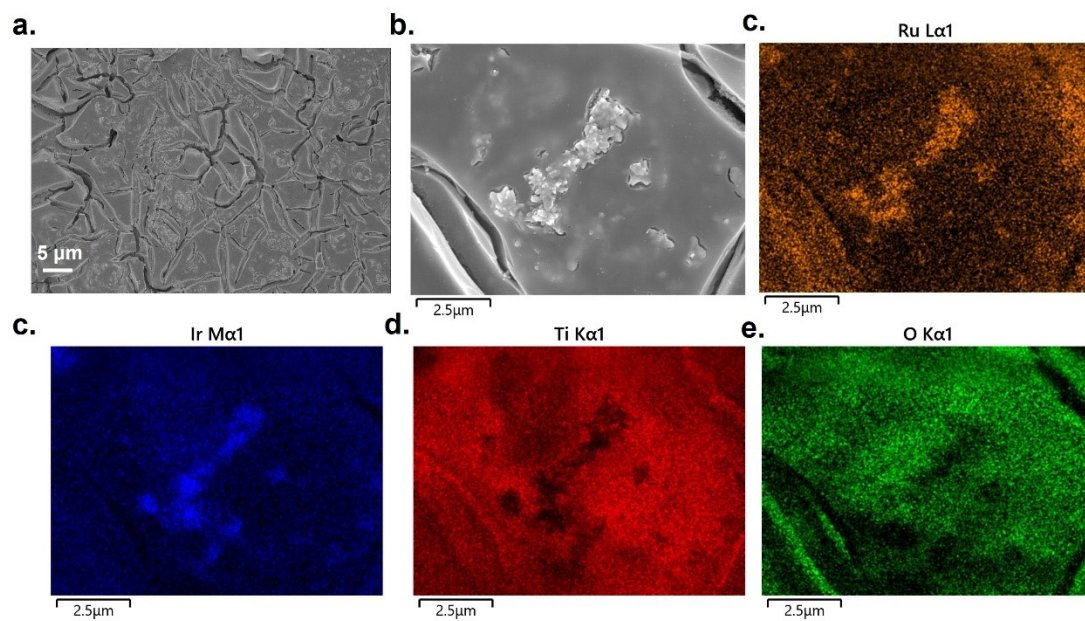


**Figure S26 | Morphology characterization of fresh Ru-IrO<sub>2</sub>-DSA anode.** a) The SEM images of fresh DSA and b-e) the corresponding EDS images.

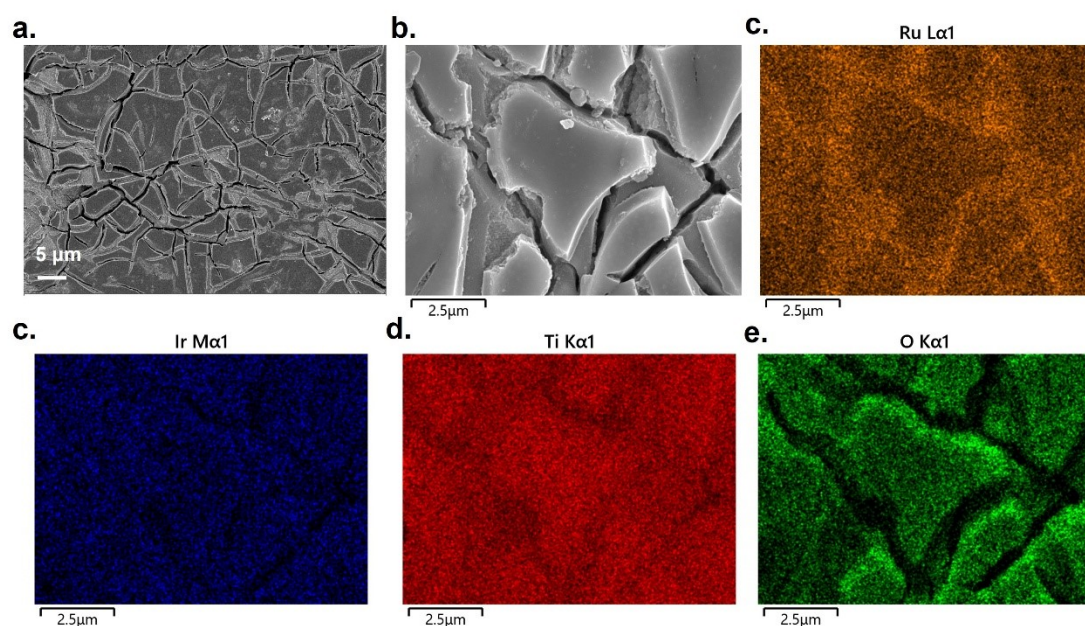


**Figure S27 | Morphology characterization of used Ru-IrO<sub>2</sub>-DSA anode.** a) The SEM images of used DSA and b-e) the corresponding EDS images. We can see the main component of the DSA (Ir and Ru) was not destroyed as confirmed by the EDS.

Note:

The detection electrode was subjected to repeated TEMPO-Silica and electrolyte cycling experiments and was reused at least ten times. After each use, it was cleaned by ultrasonic treatment in acetone and water, respectively. EDS analysis confirmed that the main components of the DSA electrode (Ir and Ru) remained intact, indicating no significant degradation of the electrode.

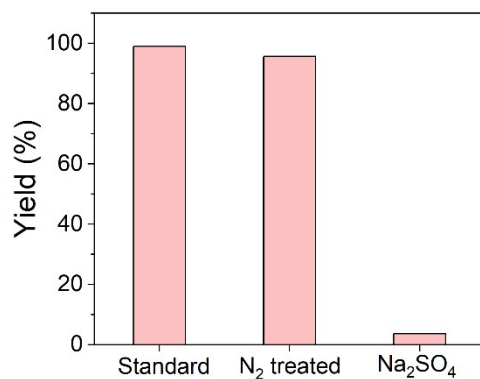


**Figure S28 | N<sub>2</sub>-treated experiment and halogen-free experiment.** For the N<sub>2</sub>-treated experiment, the electrolyte composition was identical to that of the standard reaction conditions, but the solution was bubbled with N<sub>2</sub> for 30 mins to eliminate the influence of dissolved oxygen. For the halogen-free experiment, 3.0 M NaCl and 0.01 M NaBr were replaced with 2.0 M Na<sub>2</sub>SO<sub>4</sub>. Anode: DSA (1 cm<sup>2</sup>). Cathode: Nickel foam (1 cm<sup>2</sup>).

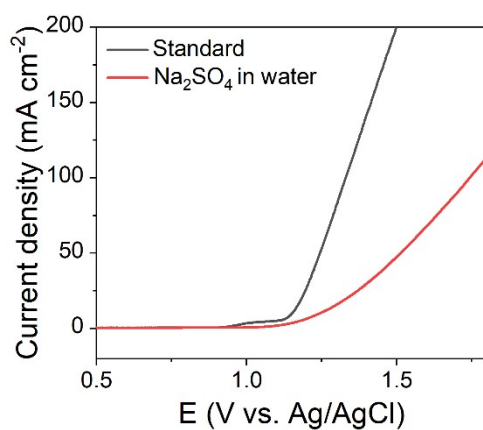


**Figure S29 | The linear sweep voltammograms of DSA.** Analyzed solutions: 3 M NaCl and 0.01 M NaBr in 10mL of water solvent. Ag/AgCl was used as reference electrode and nickel foam was used as counter electrode. The scan rate was 20 mV/s. For the halogen-free experiment, 3.0 M NaCl and 0.01 M NaBr were replaced with 2.0 M Na<sub>2</sub>SO<sub>4</sub>.

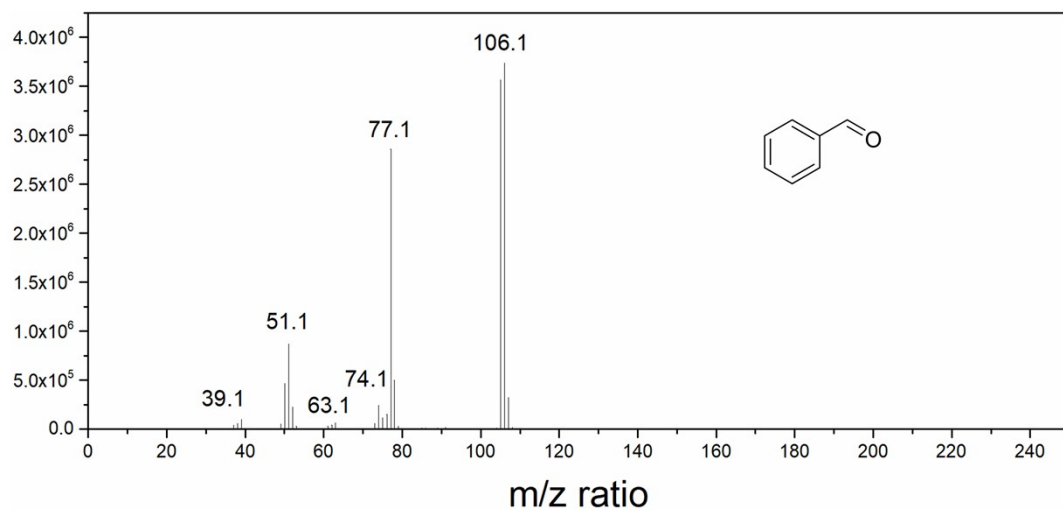


**Figure S30 | GC-MS of benzaldehyde.**

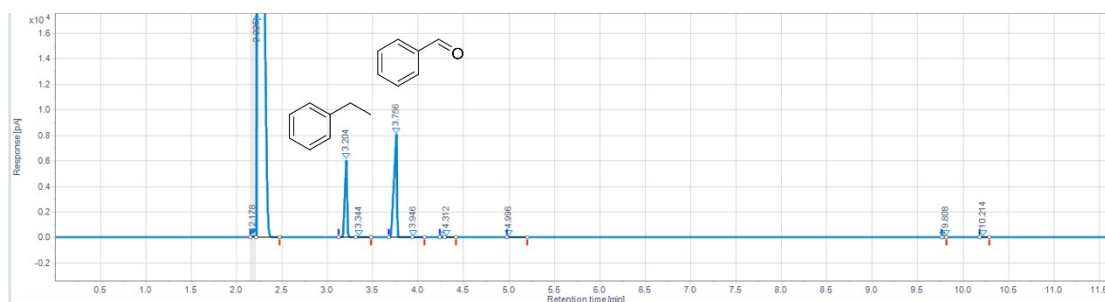


**Figure S31 | Gas chromatogram for benzyl alcohol oxidation at standard reaction condition.**

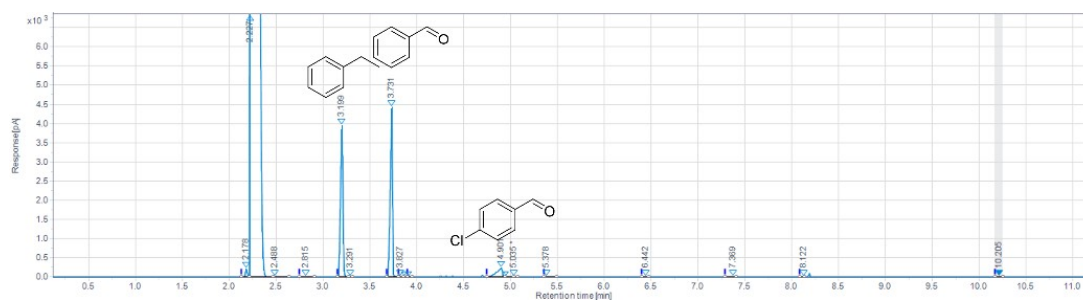


**Figure S32 | Gas chromatogram for benzyl alcohol oxidation reaction with an increased charge.** Reaction solutions: 0.5 mmol of benzyl alcohol in 1 mL CH<sub>2</sub>Cl<sub>2</sub> with 5 mol% TEMPO (4 mg), then adding 14 mL water with 3M NaCl and 0.01 M NaBr. Anode: DSA (1 cm<sup>2</sup>). Cathode: Nickel foam (1 cm<sup>2</sup>). The current density is 100 mA/cm<sup>2</sup> and the total charge passed is 4 F/mol.



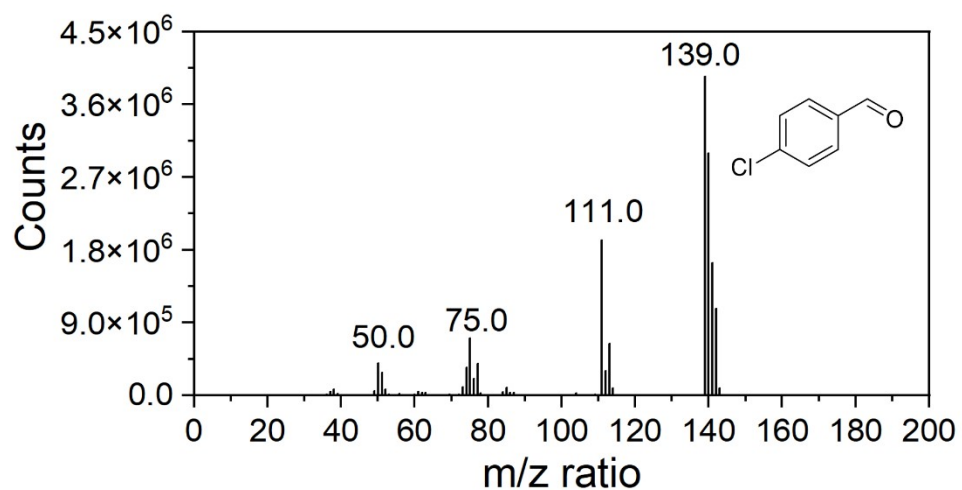


**Figure S34 | GC-MS of p-chlorobenzaldehyde.**

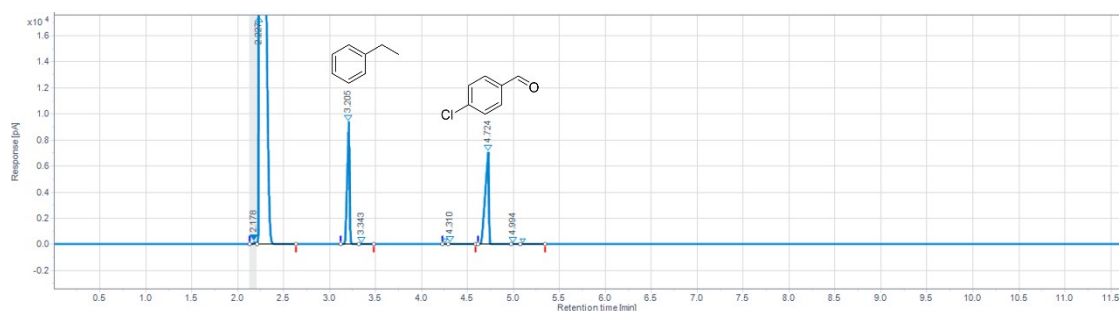


**Figure S35 | Gas chromatogram for p-Chlorobenzyl alcohol oxidation at standard condition.**

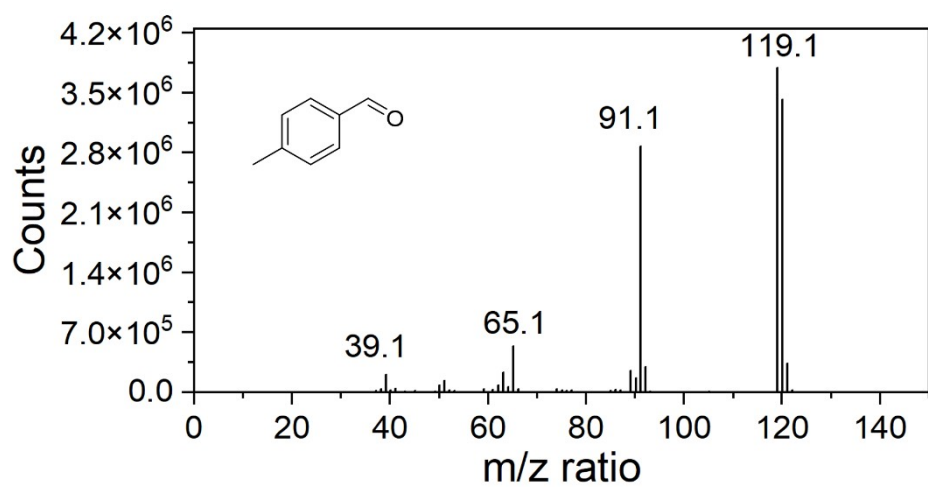


Figure S36 | GC-MS of p-methylbenzaldehyde.

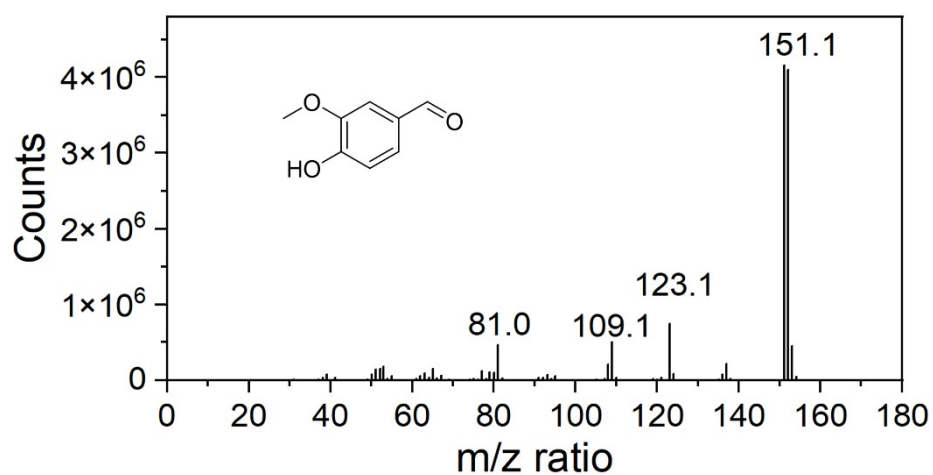
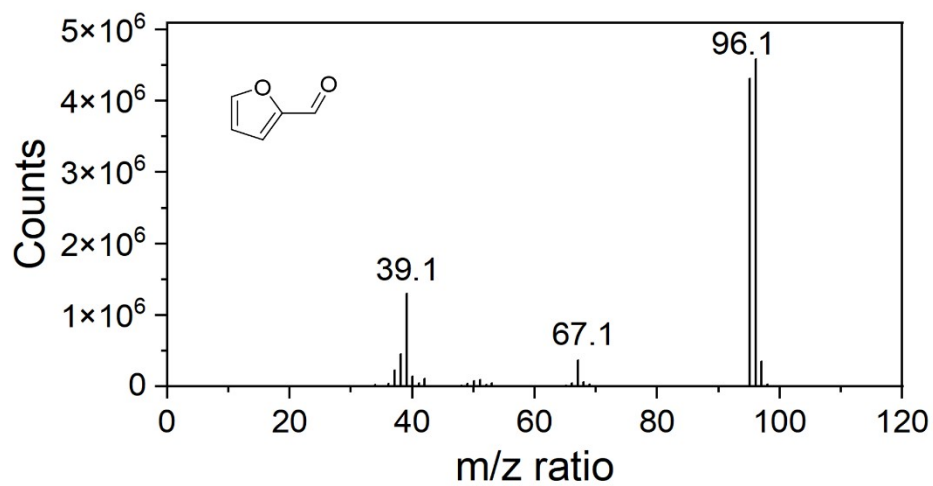
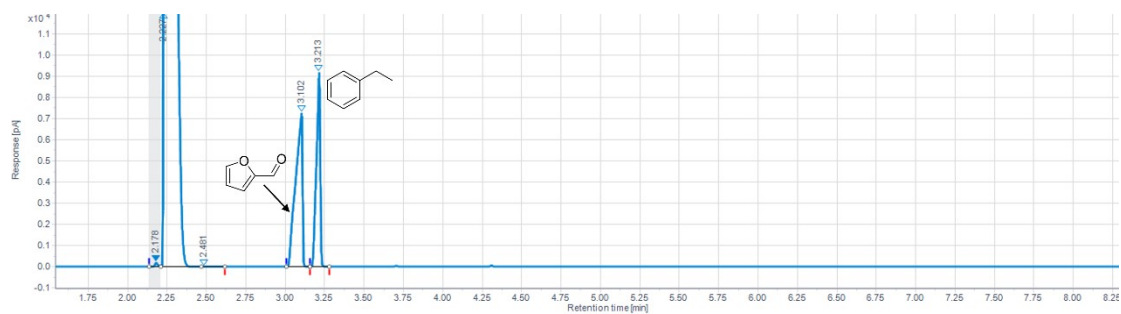


Figure S37 | GC-MS of Vanillin.



**Figure S38 | GC-MS of 2-Furaldehyde.**



**Figure S39 | Gas chromatogram for Furfuryl alcohol oxidation at standard reaction condition.**

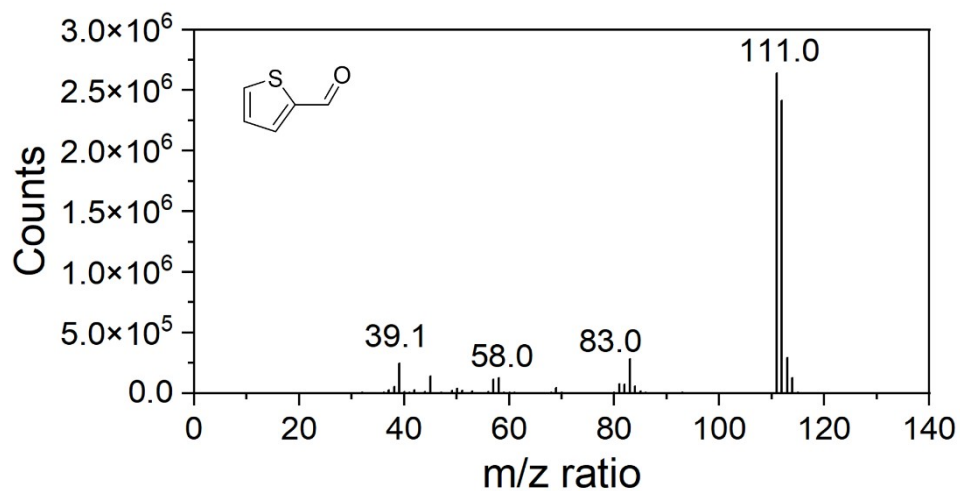


Figure S40 | GC-MS of 2-Thienaldehyde.

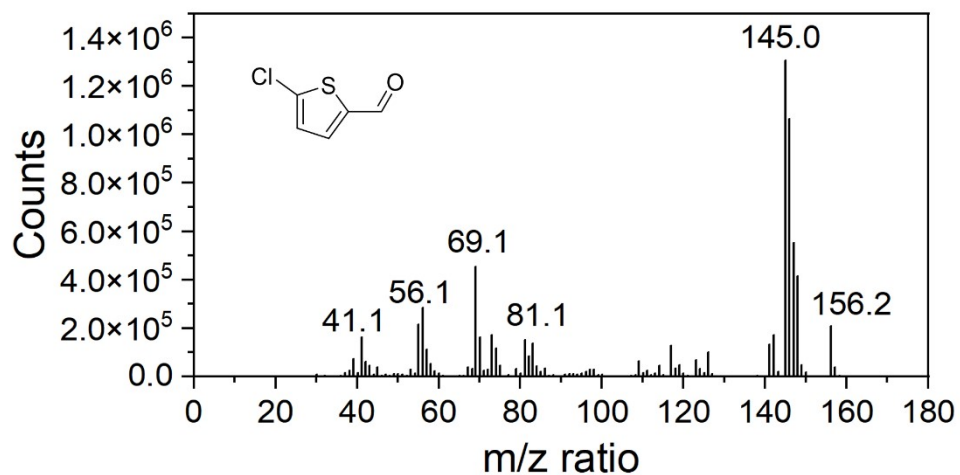


Figure S41 | GC-MS of 5-Chlorothiophene-2-carbaldehyde.

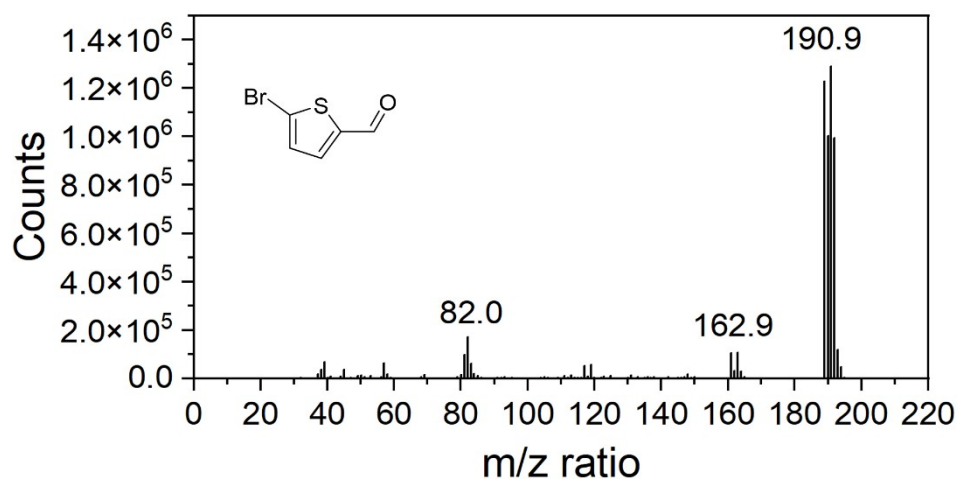
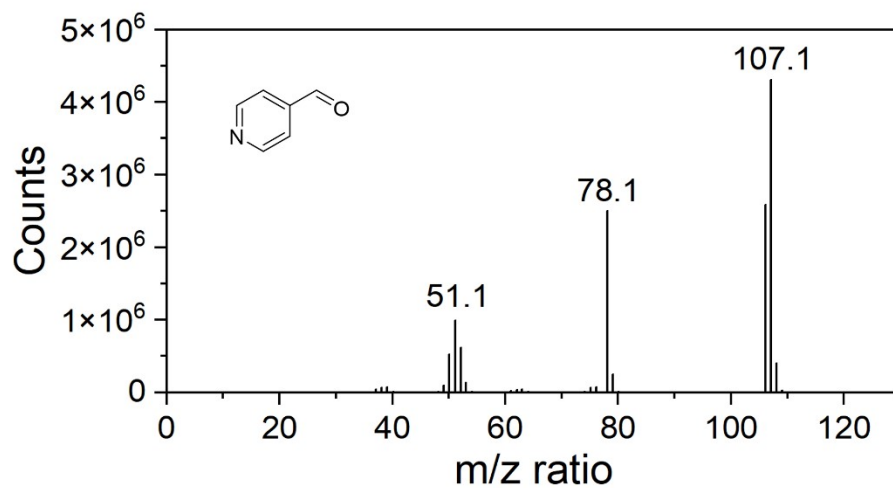
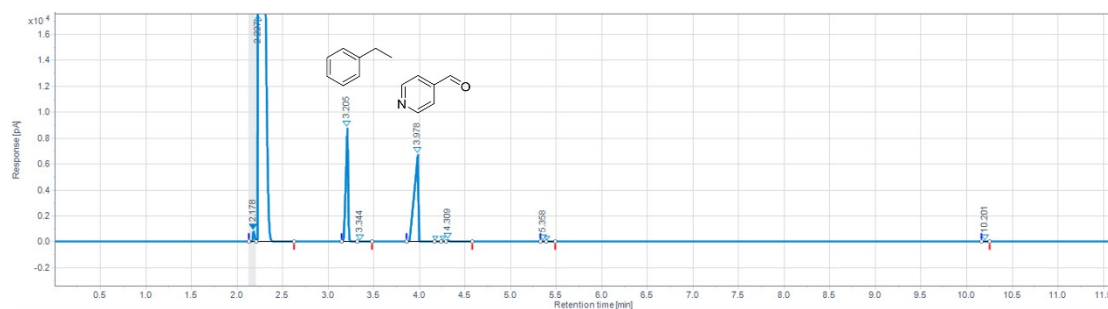


Figure S42 | GC-MS of 5-Bromo-2-thiophenecarbaldehyde.



**Figure S43 | GC-MS of 3-Pyridinecarboxaldehyde.**



**Figure S44 | Gas chromatogram for 3-Pyridinemethanol oxidation at standard reaction condition.**

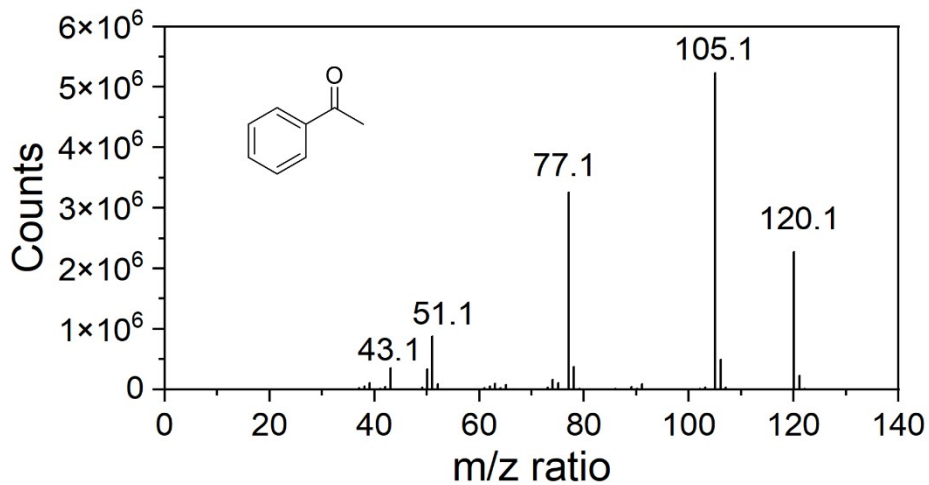


Figure S45 | GC-MS of acetophenone.

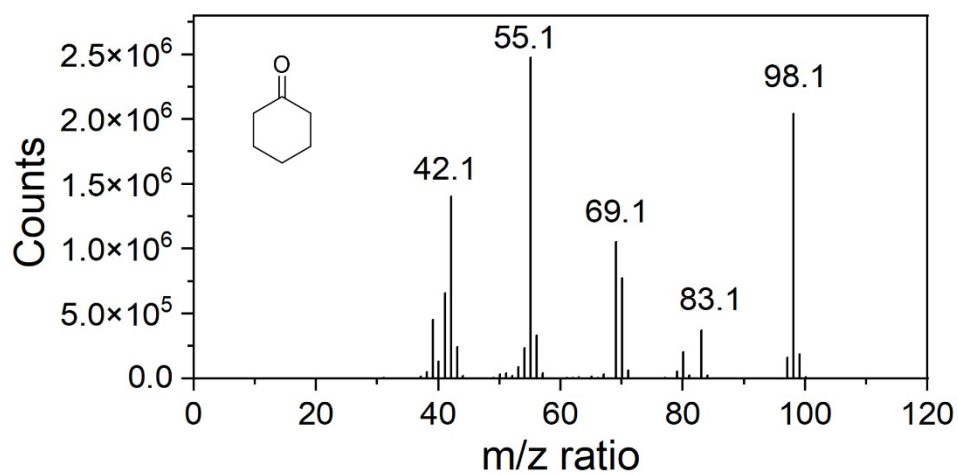


Figure S46 | GC-MS of Cyclohexanone.

## Reference

- [1] H. Zhang, L. Fu, H. Zhong, “Silica gel-supported TEMPO with adsorbed NO<sub>x</sub> for selective oxidation of alcohols under mild conditions” *Chin. J. Catal.* **2013**, *34*, 1848–1854.
- [2] T. Fey, H. Fischer, S. Bachmann, K. Albert, C. Bolm, “Silica-Supported TEMPO Catalysts: Synthesis and Application in the Anelli Oxidation of Alcohols” *J. Org. Chem.* **2001**, *66*, 8154–8159.
- [3] T. Lin, M. Cai, H. Chen, Y. Mo, “Selective electrosynthesis of aldehydes at industrially relevant current densities *via* tandem electrochemical–chemical catalysis” *Green Chem.* **2024**, *26*, 11290–11302.
- [4] R. Shi, X. Zhang, C. Li, Y. Zhao, R. Li, G. I. N. Waterhouse, T. Zhang, “Electrochemical oxidation of concentrated benzyl alcohol to high-purity benzaldehyde via superwetting organic-solid-water interfaces” *Sci. Adv.* **2024**, *10*, eadn0947.
- [5] T. Raju, S. Manivasagan, B. Revathy, K. Kulangiappar, A. Muthukumar, “A mild and efficient method for the oxidation of benzylic alcohols by two-phase electrolysis” *Tetrahedron Lett.* **2007**, *48*, 3681–3684.
- [6] A. J. Bosco, S. Lawrence, C. Christopher, S. Radhakrishnan, A. A. Joseph Rosario, S. Raja, D. Vasudevan, “Redox-mediated oxidation of alcohols using Cl<sup>-</sup>/OCl<sup>-</sup> redox couple in biphasic media” *J. Phys. Org. Chem.* **2015**, *28*, 591–595.
- [7] T. Inokuchi, S. Matsumoto, S. Torii, “Indirect electrooxidation of alcohols by a double mediatory system with two redox couples of [R<sub>2</sub>N<sup>+</sup>=O]/R<sub>2</sub>NO<sup>•</sup> and [Br<sup>•</sup> or Br<sup>+</sup>]/Br<sup>-</sup> in an organic-aqueous two-phase solution” *J. Org. Chem.* **1991**, *56*, 2416–2421.
- [8] Y. Chen, S. Wang, Z. Xu, Y. Wang, J. He, K. Li, J. Wang, L. Liu, L. Ren, S. Li, Z. Zhang, X. Zhong, J. Wang, “Boosting electrocatalytic alcohol oxidation: Efficient d–π interaction with modified TEMPO and bioinspired structure” *AIChE J.* **2025**, *71*, e18662.